

THE PENNSYLVANIA STATE UNIVERSITY
SCHREYER HONORS COLLEGE

DEPARTMENT OF BIOCHEMISTRY AND MOLECULAR BIOLOGY

CONSTRUCTION AND CHARACTERIZATION OF A CYAN FLUORESCENT-
EXPRESSING POLIOVIRUS

ZIWEI YANG
SPRING 2018

A thesis
submitted in partial fulfillment
of the requirements
for a baccalaureate degree
in Biochemistry and Molecular Biology
with honors in Biochemistry and Molecular Biology

Reviewed and approved* by the following:

Craig E. Cameron
Professor, Eberly Family Chair of Biochemistry and Molecular Biology
Honors & Thesis Supervisor

Joyce Jose
Assistant Professor of Biochemistry and Molecular Biology
Faculty Reader

Wendy Hanna-Rose
Interim Department Head for Biochemistry and Molecular Biology

* Signatures are on file in the Schreyer Honors College.

ABSTRACT

Positive-strand RNA viruses are well known agents that cause diseases in humans, animals and plants.¹ This includes West Nile virus, Severe Acute Respiratory Syndrome (SARS) Virus, Chikungunya virus and most recently Zika virus.² Due to concerns regarding the potential threat to the public health posed by these viruses, production of effective antiviral therapeutics against RNA viruses has become an increasingly hot topic. However, this requires us to have a comprehensive understanding of the characteristics and mechanisms by which viruses replicate in cells. One particular aspect of this is the cell-to-cell variability of infection by RNA viruses due to viral genetic variation. To uncover this unique feature of RNA virus infection, our laboratory uses poliovirus (PV) as a model RNA virus to investigate and characterize the kinetics of viral replication.

My goal is to unravel the distinct trait of viral replication in different individual cells due to the intrinsic diversity of each virus population. All positive-strand RNA viruses exist as a population of genetically distinct variants that leads to different outcomes of infection in individual cells of a tissue or organ.³ However, few laboratories characterize this between-cell variability of infection.^{32, 33} To do this, a single cell platform must be employed, which requires the use of a fluorescent reporter virus that can be utilized for live-cell imaging.¹¹

Here, I will explain in detail how a recombinant cyan fluorescent protein-expressing PV, CFP-PV, was designed and produced for such purpose. Initial characterizations of the virus using fluorescent imaging suggest that the engineered virus is able to generate robust cyan fluorescent signal upon infection in HeLa cells. In addition, according to the plaque assay results, the CFP-

PV demonstrates growth properties stronger than the currently available GFP-PV reporter virus in the Cameron lab by one log order, indicating that the reporter gene engineered into the viral construct does not affect the virus's infectivity at large. This shows that the reporter virus produced in this work functions well as expected and is ready to be used for single-cell analysis, which aims to characterize the between-cell variability of infection by observing each infection event individually in a population of infected cells.

TABLE OF CONTENTS

LIST OF FIGURES	iii
LIST OF TABLES	iv
ACKNOWLEDGEMENTS	v
Chapter 1 Introduction	1
Viral Infection and Viral Genetic Variation	1
Chapter 2 Design of the Reporter Virus	6
Chapter 3	9
QIAEX Purification for PCR Product and Ligation Product.....	10
Transformation of CFP _{PV} -PV Plasmid into SURE Cells.....	11
Chapter 4 Results	17
Producing the CFP _{PV} via PCR.....	17
Chapter 5	26
Chapter 6.....	29
BIBLIOGRAPHY.....	31

LIST OF FIGURES

Figure 1. Poliovirus Genome Structure	3
Figure 2. PCR for CFP _{PV} gene. Size of the CFP _{PV} gene is 729bp.....	17
Figure 3. Sal-I & Xho-I Digest of CFP _{PV} gene and PV vector. Single bands were observed in both PCR and vector lanes, with no unexpected bands visible. Sal-I and Xho-I restriction enzymes were used for both digestion reactions. The faint band in the cut vector lane that corresponds to 0.7kb is the spill-over DNA from the PCR lane.....	18
Figure 4. Ligation between the CFP _{PV} gene and the PV construct. A spectrum of bands is visible in the ligation product lane, indicating self-ligation or multimerization between the PCR gene inserts. No vector self-ligation band is visible, showing that the de-phosphorylation of the vector was successful.	20
Figure 5. Sal-I and Xho-I Digest (MINI Screen). Four samples obtained from the ligation product plate yielded the characteristic double bands by digesting the extracted DNA with Sal-I and Xho-I. No unexpected bands are visible, showing that the CFP _{PV} -PV product is pure.	22
Figure 6. CFP _{PV} -PV RNA Viral Construct. Quality of the viral RNA was checked after being transcribed from the DNA construct.....	23

Figure 7. Bright Field and Fluorescent Imaging of the Cells. (A) Bright field imaging of the cells exhibits all the cells on the six-well plate. (B) Fluorescent imaging of the cells reveals only cells that contain fluorescent viruses.24

Figure 8. Plaque Assay. Plaque assay was performed to determine the viral titer of the fluorescent virus. Viral titer was determined to be 1.1×10^8 PFU/mL—similar to that of the wild type poliovirus.25

ACKNOWLEDGEMENTS

My undergraduate research experience has been an incredible adventure filled with innumerable challenges and surprises, and I would not have been able to do it without the support from various important people in my life.

First, I wish to express my deepest gratitude to my amazing mentor, Dr. Craig E. Cameron. Thank you for recognizing in my potentials and for showing me the way to a career of research when I didn't know what I wanted for my future. Your passion and spirit as a scientist and your continuous support for my training as a mentor have tremendously influenced me and have led me onto this amazing path. Thank you!

I also want to thank my labmates Dr. Suresh D. Sharma, Dr. Andrew Woodman, Dr. Wu Liu, Dr. Jamie Arnold, Calvin Yeager, Henry Hsiung, David Aponte Diaz, Jacob Perryman, etc. Thank you for your endless support during this project. Special thanks to Dr. Suresh Sharma, for his patient mentoring, supervising, and helping me develop my skills as a researcher throughout the entire project. I wouldn't have gone this far without your help.

Special thanks to the Penn State BMB department and the Schreyer Honors College as well for enabling this journey.

Finally, I want to thank my friends and family for their unwavering encouragement. Their patience and inspiration are what sparked my interest in science in the first place. Furthermore, their continued and unconditional support have always kept me going even during my hardest times. None of this would ever be possible if it wasn't for them. Thank you and I love you!

Chapter 1

Introduction

Viral Infection and Viral Genetic Variation

Viruses are small infectious agents that rely on living cells to replicate and proliferate. Viruses can infect organisms in all domains of life, including animals, plants and microorganisms.⁴ Like with all organisms, replication is the key to viruses' survival. In addition, although viruses have a non-cellular structure unlike most other organisms, they still use the basic genetic material that is universal for all living beings (DNA/RNA) to direct their biological processes within cells, including viral replication.⁵ Therefore, viral genetic information is at the center of viral infection.

Since RNA viruses mainly exist as a population of genetically distinct variants, genomic variation between different individual virus could lead to different outcomes of infection in cells of a tissue or organ.^{6,7,8} As these differences in infection may reveal important features of viral infection, characterization of this between-cell variability of infection has become an important topic for studying viruses.⁹ However, because the traditional population approach used in virology often masks these important characteristic variations of viral infection in different individual cells, analyzing the virus-host interaction at the single cell level becomes an important

method for unraveling these unique traits.^{10, 11} In order to do this, a fluorescent reporter virus is needed for use in the single cell platform.

Viral Infection Cycle

Poliovirus, a member of the *Enterovirus* genus in the *Picornaviridae* family, is a small positive sense, single stranded RNA virus with a genome size about 7500 nt long and a nonenveloped icosahedral virus structure that consists of 60 copies of each of the four capsid proteins, VP1, VP2, VP3, and VP4.^{12, 13} Upon viral entry, the positive sense viral RNA is uncoated and acts directly as mRNA and use the host ribosome to initiate viral translation in producing the viral polypeptide under the control of the internal ribosome entry site (IRES).^{14, 15} Structural organization of these viral proteins within the polypeptide can be seen from the genetic map of the viral genome shown in figure 1. The viral polypeptide is then cleaved by virus-encoded proteases, 2A^{pro} and 3C^{pro}, into functional viral proteins.^{16, 17} In addition, the 2A^{pro} also mediates cleavage on the host cell eukaryotic translation initiation factor 4G (eIF4G), which is involved in the eukaryotic translation initiation. This effectively curbs the host protein synthesis because eIF4G is required for the 5' cap-initiated mRNA translation.^{18, 19} However, the 2A^{pro}-mediated cleavage does not affect the IRES-initiated viral translation, permitting the production of viral polypeptide.²⁰ Upon translation of the whole viral polypeptide, which contains both a structural and a non-structural protein region, the 2A^{pro} protease will first mediate a cis-cleavage at the linkage region between the VP1 and 2A, separating the P1 precursor that encodes structural proteins (VP1, VP2, VP3, VP4) from non-structural regions (P2-P3 region).²¹ Later, the 2A^{pro} and 3C^{pro} proteases together will cleave the viral polypeptide to produce

functional proteins that are essential for viral replication.^{22, 23} This includes proteins necessary for the replication-organelle synthesis (non-structural protein). This process is completed upon initial translation phase, which occurs within 1-hour post infection, in order to prepare for the genome replication in the following phase.^{24, 25} After this small-scale initial translation phase, genome replication begins.²⁶ When sufficient amount of viral genome is synthesized, additional protein translation will take place at about 4-hour post infection, producing proteins necessary for virion assembly.²⁷ Afterwards, virion assembly will take place, followed by viral egress using cell lysis as the primary means. It has been observed that cytopathic effects within infected cells occur at 4 to 6-hour post infection and each infected cell could produce up to 10,000 viral particles upon lysis.^{28, 29} In order to characterize these viral infection processes to better understand the dynamics and the intrinsic heterogeneity of viral replication due to cellular and viral genetic variation, single-cell analysis must be utilized.³⁰

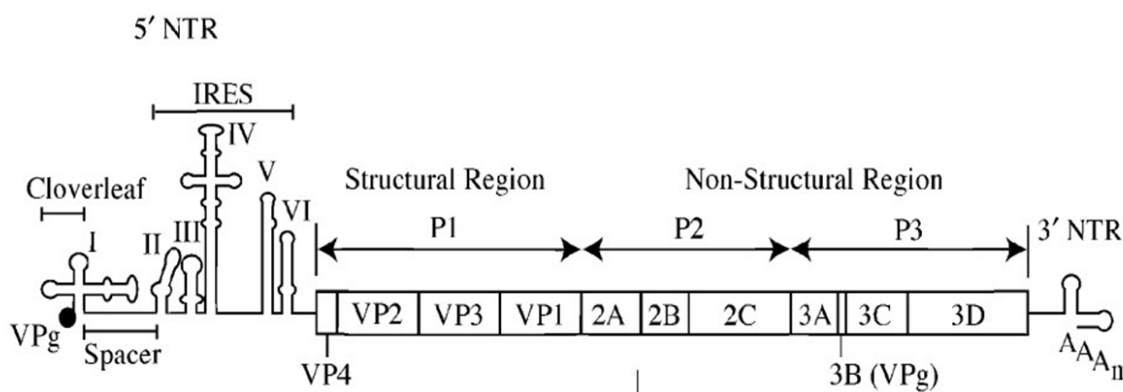


Figure 1. Poliovirus Genome Structure

Single-Cell Analysis

The traditional population approach used in the field of virology for characterizing viral infection relies on the quantification of the infectious viral particle concentrations via plaque assay or evaluation of the virion production kinetics via single-step growth analysis.³¹ Both methods tend to mask important characteristics of viral infection such as the between-cell

variability that arises from viral and cellular genetic variation.¹¹ This could greatly hinder our ability to perceive how different viruses are behaving within each individual cell. For example, if during an infection, 60% of the progeny virus particles are produced from only 10% of all the infected cells, it could be indicating that virus or host cell factor expression varies in different cells. While this could demonstrate a significant variation in viruses' replication fitness in individual cells, a population method would preclude such observation and the subsequent conclusion because it would attribute the production of the virions during the infection to all infected cells and yield an average "virion produced per cell" result (pfu/ml). In addition, using the population approach could also complicate the interpretation of results from drug treatments. For example, if an effective antiviral drug could eliminate all the highest-yielding infections, such drug could only generate a two-fold reduction to the infection outcome at the population level, creating a false impression that the drug is ineffective at curbing the virus infection.¹¹

However, using a single-cell platform would help avoid such issue as it aims to analyze all the infection events individually.^{32, 33} Therefore, to characterize the viral infection kinetics in single cells, our lab has developed a high-throughput, microfluidics-based platform for use in fluorescent microscopy. Using this platform, we were able to investigate thousands of poliovirus infection events individually under different experimental parameters such as cell cycle, multiplicity of infection, and presence of antiviral drugs. The key is that each reporter molecule generated by the engineered reporter virus could serve as a signal that reflects the replication rates of the virus within infected cells, and when those signals are collected and integrated into a plot, a single-step growth curve can be produced. Within this curve, each infection event's starting time point, viral replication rate, and amount of virus produced can be quantified and be used to unravel the distinct traits of infection within individual cells. However, in order to do

this, a reporter virus must first be created via genetic approach as a tool for use in the single-cell platform. Such engineered virus needs to be designed to generate the reporter signal as quickly as possible upon infection in order to enable us to maximally characterize the infection process.

Chapter 2

Design of the Reporter Virus

Design of the Original Reporter Virus

As explained in previous chapter, an ideal reporter virus design should allow the virus to produce the reporter signal as early as possible upon infecting a cell. Because the reporter signal directly serves to reflect the growth rate of the virus within cells, the earlier we could obtain such signal, the earlier the characterization can begin. Delay of the signal due to slow viral cleavage (required for protein release) or protein folding could limit the extent of such characterization. With this goal in mind, our lab has developed and produced a green fluorescent-expressing poliovirus, by inserting a poliovirus-optimized green fluorescent protein (GFP_{PV}) gene into the virus construct between the VP1 and 2A regions. It is thought that as one of the first viral proteins that becomes active upon translation, the $2A^{pro}$ allows an immediate cis-cleavage at the GFP_{PV} region and releases the GFP at the fastest rate after the protein is translated, enabling the fluorescent signal to be generated at the earliest time point post infection. However, a later study suggests that because the GFP_{PV} is attached to both VP1 and 2A regions while $2A^{pro}$ only cleaves at the GFP_{PV} -2A linkage, a secondary cleavage by the $3C^{pro}$ is required for the full release of the GFP_{PV} from the VP1 region. Since this secondary cleavage by $3C^{pro}$ has a long duration period, a significant fluorescent delay will result upon infection by this reporter virus. Such a delay will largely hinder our ability to characterize the early infection events that occurs during the poliovirus replication cycle. For example, since the fluorescent signals cannot be produced by

this virus before 4-hour time point post infection, it prevents any quantitative characterizations of the initial translation phase, whose occurrence is prior to 2-hour time point post infection.

Therefore, to better examine these early events, a new reporter virus is needed, a virus whose fluorescent rate is significantly improved.

Design of the New Virus

To improve the speed at which the fluorescent signal can be produced, a novel virus design was developed in which a cyan fluorescent protein encoding gene (CFP_{PV}) is fused at a site such that the fluorescent reporter can be released from the viral polypeptide by a single viral cleavage upon translation, without involving secondary cleavage. This new site is located prior to the VP4 region at the 5' end of the viral genome. Following the translation of the polypeptide, the viral 3C^{pro} will mediate a trans-cleavage at the CFP_{PV}-VP4 linkage site, releasing the fluorescent reporter from the polypeptide and allow it to freely fold into its functional structure. This optimally allows the fluorescent rate to be improved because the fluorescent protein folds at a higher efficiency when it's free and unbound. In order to make the construct viable for producing infectious reporter virus, various changes were made to the viral genome and the fluorescent protein gene. First, the fluorescent protein gene used for making the reporter virus, the cyan fluorescent protein (CFP), was optimized to the poliovirus genome (CFP_{PV}) such that its AT base pair vs. CG base pair ratio (GC content) is consistent with that of the viral genome. This prevents the CFP gene insertion from changing the infectivity of the virus, as a stable GC content is critical to maintaining important biological properties of the viral genome such as its thermal stability.⁴²

Since the CFP_{PV} is designed to be fused at the 5' end of the viral genome, implementing an artificial restriction recognition site at the corresponding region becomes essential because this enables site-specific insertion of the gene. In addition, an M-G-A-Q amino acid motif, whose encoding nucleotide sequence induces translation, was also engineered into the viral genome prior to the restriction site in order to promote translation initiation at the new site. On the other hand, the natural translation start site was inactivated via deletion of the original start codon to select against translation initiation at this location. Following this modification, the CFP_{PV} gene was engineered into the 5' end of the viral genome via site-specific insertion to yield the recombinant construct, which is then used to produce the infections reporter virus.

Chapter 3

Materials and Methods

PCR for the CFP_{PV} Gene

For the PCR reaction that amplifies the CFP_{PV} gene, 35µl of 10x Thermopol buffer, 35µl of 3mM dNTP mix, 35µl of 5µM forward primer (5` - GCG GAA TTC GTC GAC ATG GTG TCC AAA GGA -3`), 35µl of 5µM reverse primer (5` - GCG AGA TCT CTC GAG CTT GTA GAG CTC GTC -3`), 35µl of DNA template (5ng/µl), 171.5µl of ddH₂O and 3.5µl of deep vent enzyme were added to the reaction mixture. The PCR reaction was then carried out under such condition: first incubated the mixture at 95°C for 1 minute; then underwent three 3-step incubation cycles, which includes incubation at 95°C for 1 minute during step one, incubation at 50°C for 1 minute during step 2, and incubation at 72°C for 1 minute during step 3; third, the mixture was put through thirty 3-step incubation cycles, which includes incubation at 95°C for 1 minute during step 1, incubation at 57°C for 1 minute during step 2, and incubation at 72°C for 1 minute during step 3; finally, reaction mixture was incubated at 72°C for 10 minutes. After PCR, the target CFP_{PV} gene was purified from the mixture via gel purification using SeaKem Agarose gel.

QIAEX Purification for PCR Product and Ligation Product

The purified CFP_{PV} gene and the PV construct was then digested using Sal-I and Xho-I restriction enzymes to create the complimentary sticky ends for gene insertion. After digestion, the CFP_{PV} insert and the PV construct (as well as the ligation product in later steps) was then purified from the reaction mixture using QIAEX purification. 3 volumes of the QX I solubilization buffer to 1 volume of PCR sample was then added to the tube (for ligation product, 2 additional volumes of water were also added). Check that the color of the sample mixture is yellow. Afterwards, QIAEX II beads were re-suspend by tube-flicking. 2 µl of QIAEX II beads suspension per 1 µg of DNA (2.5 µl minimum) was then added to the tube and mix at room temperature by inverting and flicking the tube. Sample was then centrifuged for 30 second and supernatant was removed. Washed the pellet twice with 500 µl of Buffer PE (4 parts 100% EtOH, 1 part 10 mM Tris, pH 7.5 – 8.0). The pellet was then incubated at 37°C until it became white. The PCR product pellet was then re-suspended in 30 µl of T₁₀E_{0.1} and incubated at 37°C for 5 minutes to elute the DNA (ligation product pellet was incubated at 65°C for 5 minutes). Centrifuged sample at 16,000rpm for 1 min. Supernatant was then removed, transferred to a clean tube, followed by a second centrifugation. The double-digested, QIAEX purified CFP_{PV} insert and PV construct was then ligated using T7 DNA ligase to produce the CFP_{PV}-PV recombinant viral DNA construct, after which the ligation product was also QIAEX purified.

Competent Cells

SURE competent cells (Stop Unwanted Rearrangement Events) were inoculated with 100 ml of NZCYM containing the Tet-20 antibiotics. The cells were then grown at 37°C to an OD_{600nm} of 0.4. 50 ml of CaCl₂ solution (4.4 g of CaCl₂, 75 ml of 100% glycerol, 1.7 g of PIPES, and pH7) and four 30 ml corex tubes (pre-sterilized) were chilled for use in future steps. Aliquoted culture into corex tubes and centrifuged at 1600 G for 7 minutes at 4°C, then discarded the supernatant. Pellets were then re-suspended (5 mL each pellet) in a total of 20ml ice-cold CaCl₂ solution and the contents were combined into 2 tubes (10 mL per tube). Re-suspension was performed very gently and all SURE cells were kept on ice throughout the process. Cells were then centrifuged for 5 minutes at 1600 times g and at 4°C. Supernatant was then discarded and pellets were re-suspended in a total of 20 ml ice-cold CaCl₂ solution (10 ml for each pellet). The re-suspension mixture was kept on ice for 2 hours. Cells were again centrifuged for 5 minutes at 1600 G and at 4°C, then discarded the supernatant and re-suspended pellets in a total of 8 ml ice-cold CaCl₂ solution (4 ml for each pellet). Cells were then dispensed into pre-chilled, sterile polypropylene tubes (~ 350 µl), froze immediately in dry ice and stored in the freezer for future steps of the project (transformation).

Transformation of CFP_{PV}-PV Plasmid into SURE Cells

Aliquoted 5 ng of DNA (5 ul of ligation reaction) into a sterile 1.5 ml Micro centrifuge tube and placed the tube on ice. One hundred microliter of the competent cells prepared in previous steps was then thawed on ice and dispensed into test tubes that contained DNA

immediately after cells were thawed. Gently swirled the tubes to mix, then placed the tubes on ice for 10 minutes. Heat shocked cells by placing tubes from ice into a 37°C water bath for 1 minute. Following heat shock, cells were immediately placed on ice for 2 minutes. 900 µl of SOC (pre-warmed at 37°C) and Dextrose solution (final Dextrose concentration is 4%) were then added to the tube, followed by incubation at 37°C for 1 hour. Inoculated 10% of transformed culture on plates containing Amp-50 antibiotics (for PV vector), then incubated the plates for 16 hours at 30°C (for SURE cells).

Mini Prep After Extracting the Colonies from Transformation

Single colonies from the ligation plate were inoculated the night before the mini prep and was incubated at 37°C overnight under constant shaking (250 rpm). Centrifuged 1.5 ml of cultures for 1 min in a 1.7 ml centrifuge tube, then discarded the supernatant. Re-suspended each pellet in 100 µl Buffer P1 (1µl RNase per 100 µl P1). 100 µl of Buffer P2 (NaOH, SDS) was then added and mixed well by inversion, followed by addition of 100 µl of Buffer P3 (KOAc) and mixed it well by inversion. Mixture was then centrifuged for 10 minutes at 4 °C, which helped pellet out the SDS, proteins, cell wall and chromosomal DNA. Transferred the supernatant to another tube and added 900 µl of 100% ethanol to the supernatant. Because of the Na⁺ and K⁺ ions, the plasmid will become neutral and pellet out when spun. The supernatant mixture (added with ethanol) was then mixed via vortexing and spun for 1 min. Ethanol was then removed. Washed the tube content with 750 µl of 70% ethanol. This step serves to remove the Na⁺ and K⁺ ions, while ethanol will keep DNA pelleted. Centrifuged the mixture for 1 minute, removed the ethanol, then air dried the content for 2 minutes. After drying, the content was re-

suspended in 50 μ l TE (Tris and EDTA, which chelates the divalent metals so any trace nucleases will not cleave DNA). The extracted clones were then screened via Sal-I and Xho-I double digestion to select for the correct plasmid, which contains the target CFP_{PV} insert in the PV construct.

MIDI Prep of Correct CFP_{PV}-PV Plasmid (after screening the colonies)

First inoculated 100 ml of the appropriate media, each with 100 μ l of selected colonies from a transformation plate. Note that colonies were inoculated the night before the midi prep and was incubated at 37°C overnight under constant shaking (250 rpm). Cell culture was then pelleted at 6000 rpm for 10 minutes, after which the supernatant was discarded. Re-suspended each pellet in 4ml of Buffer P1 (essentially TE), then added 40 μ l of RNase A (10 mg/ml) to the mixture and transferred the mixture into an ultra-centrifuge tube. Added 4 ml of Buffer P2 (NaOH, SDS) to the tube, mixed it well via inversion, then waited for 5 minutes. 4 ml of Buffer P3 was then added and mixed well via inversion. The mixture was then pelleted at 24,000 rpm and at 4°C for 30 minutes. Next, a QIAGEN tip-100 was equilibrated with 3 ml QBT. Supernatant was added from the centrifuged mixture to a 10 mL disposable syringe attached to a wizard column and filtered the solution to the QIAGEN tip, then washed the tip twice with 10 ml of Buffer QC. Eluted the DNA from the column into a clean tube with 5 ml Buffer QF, then added 0.8 volumes (4 ml) of isopropanol to the eluted DNA and mixed by vortexing. Next, the DNA-containing mixture was pelleted at 24,000 rpm and at 4°C for 30 minutes, after which the supernatant was removed immediately and the tube was kept inverted so as not to lose the pellet. Pellet was then re-suspended in 350 μ l of sterile TE. 0.2 volumes (70 μ l) of sodium acetate (3M

NaOAc, pH 5.2) and 3 volumes (1000 μ l) of 100% ethanol was then added to the tube and mixed the contents via vortexing. The mixture was then pelleted at 6000rpm for 1 minute and the supernatant was removed. The pellet was then washed 3 to 5 times with 750 μ l of 70 % ethanol and vortexed. The mixture was then briefly centrifuged, after which the 70 % ethanol was removed, and the pellet was air dried for 5 minutes. Finally, the pellet was re-suspended in 100 μ l of sterile T₁₀E_{0.1}.

Preparing the CFP_{PV}-PV Viral RNA Genome Using T7 In Vitro Transcription

After harvesting the CFP_{PV}-PV DNA construct from selected *E. coli* colonies via midi prep, the DNA construct was linearized by Apa-I enzyme. Functional positive sense CFP_{PV}-PV RNA viral genome was then produced from the linearized DNA via T7 transcription: 7 μ l of 1M HEPES, 2 μ l of 320 mM magnesium acetate, 2 μ l of 400 mM DTT, 2 μ l of 20 mM Spermidine, 3.5 μ l of 160 mM NTPs, and 2.5 μ l of 0.02 μ g/ μ l DNA were first added to a fresh Micro centrifuge tube. The reaction mixture was pre-incubated at 37°C for 5 minutes, after which 1 μ l of 0.025 μ g/ μ l T7 RNAP was added to the heated mixture. The reaction mixture was then incubated at 37°C for 3 hours. After the 3-hour incubation, reaction mixture was pelleted at 6000 rpm for 2 minutes (to remove the magnesium pyrophosphate), followed by removal of supernatant, then 2 μ l of RQ1 DNase (1 unit/ μ l) was added to the mixture. The mixture was then incubated at 37°C for 30 minutes. Next, the reaction mixture was added to 50 μ l of LiCl (7.5 M LiCl & 50 mM EDTA) and the mixture was placed on dry ice for 10 minutes. The chilled mixture was pelleted at 14,000 rpm and at 4°C for 20 minutes, after which the supernatant was removed. 0.5 ml of 70% ethanol was then added to the mixture and was mixed via inversion. 70% ethanol was then

discarded without losing the pellet, after which the sample was briefly centrifuged and the residual ethanol was removed. The pellet was then re-suspended in T₁₀E₁ buffer.

Electroporation of Viral RNA Genome into HeLa Cells

After producing the viral RNA genome via transcription, fluorescent reporter poliovirus was produced by transfecting the RNA into HeLa cells via electroporation. 4,000,000 HeLa cells were seeded/passaged on a 100 mm plate one day before the electroporation to prepare a monolayer. On the day of electroporation, 5.6ml of the media was pre-warmed in a 15 ml tube for each electroporation reaction. Media from the monolayer plate was removed, followed by addition of 1 ml of Trypsin and the plate was then incubated at 37°C for 2 minutes. Fresh media (contained 10% FBS) was then added to the incubated plate. Next, cells were count and set to 1.2×10^6 cells for each electroporation. Media was then removed and 400 μ l of 1 x PBS was added per 1.2×10^6 cells. 5 μ l (or 10 μ g) of RNA per electroporation (1.2×10^6 cells) was the prepared and was kept on ice. 400 μ l of cells were added and re-suspended in PBS to the tube containing RNA and mixed well. RNA and cell mixture was then transferred into a sterile, 2 MM VWR electroporation cuvette, which was subsequently put into the eletroporator. The mixture was then electroporated at 0.13 kV with 500 μ FD (2 pulses were used with a pulse width of 35 ms). Once the electroporation was completed, 500 μ l of pre-warmed (at 37°C) media was added to the cuvette and the cells were transferred back into 5.1 ml of pre-warmed media.

Harvesting the Fluorescent Poliovirus

After HeLa cells were transfected with the viral RNA and reporter viruses were produced, viruses were then harvested from the cells. The cell-virus mixture was first incubated at 37°C for 48 hours, after which the media and cell debris were scraped out and collected into a 15 ml conical tube. Next, the content was frozen (via refrigeration) and thawed for three cycles to lyse the cells. The resulting mixture was then stored at -80°C.

Characterizing Viral Infectivity using Plaque Assay

After the reporter viruses were harvested, infectivity of the fluorescent poliovirus was characterized using plaque assay. 6×10^5 cells were first passaged in each well of a 6-well plate to produce a monolayer one day before the dilution. On the next day, the harvested virus solution was serially diluted by 10-fold in PBS (10^{-2} , 10^{-4} , 10^{-5} , 10^{-6} , 10^{-7}), after which the media was removed and 200 μ l of PBS was added to the mixture. Next, 100 μ l of each dilution was added to each well of the 6-well plate prepared earlier, which contains the HeLa cell monolayer. One well was left as a negative control. The plate was then incubated at room temperature for 30 minutes. Next, PBS was removed from the plate, then washed the plate with 2 ml of 1x fresh PBS. The plate was then overlaid with media and 1% agar mix. Four steps were taken to prepare the media/agar mix: first weighed out 0.2 g of low melting agarose, then added 10 ml of dH₂O to the agarose and melted the mixture in the microwave. The mixture was then incubated in a 37 °C water bath for more than 10 minutes and was added to an equal volume of pre-warmed 2 x media (+ 20% FBS, + 2% P/S). Next, aspirated all the media and placed 3 ml of media/agar mix into each well of the 6-well plate. After overlaying the plate with media and 1% agar mix, the plate was then incubated at 37 °C for 2 days. Plates were then placed in refrigerator for 15-30 minutes to solidify the agar.

r. Next, removed the agar plugs and stained the wells with 500 μ l of Crystal Violet solution, then incubated the stained wells at room temperature for 5 minutes and washed with 500 μ l of PBS. Finally, counted and recorded the number of plaques present on the plate.

Chapter 4

Results

Producing the CFP_{PV} via PCR

Reporter gene CFP_{PV} was first amplified via PCR before producing the recombinant viral construct CFP_{PV}-PV by inserting the CFP_{PV} into the poliovirus genome (PV).

As can be seen, the vibrant bands present in the PCR gel result (figure 2) suggests that the CFP_{PV} gene was successfully amplified, with no unexpected DNA products made.

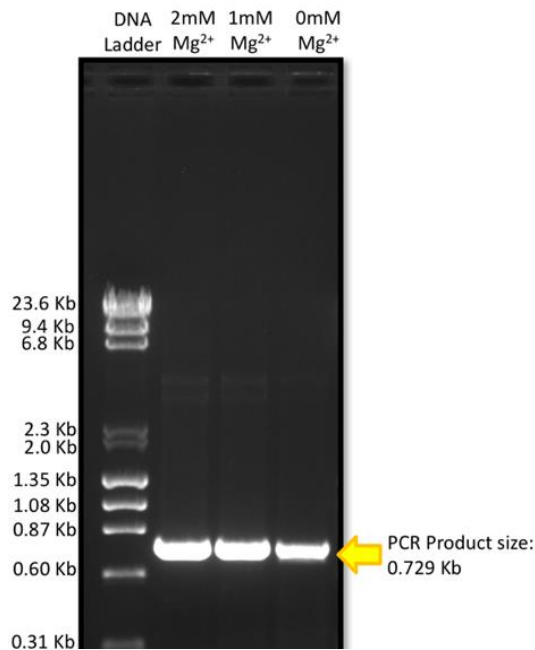


Figure 2. PCR for CFP_{PV} gene. Size of the CFP_{PV} gene is 729bp.

Restriction Digest of the CFP_{PV} Gene and PV Construct

In order to insert the CFP_{PV} gene into the 5' end of the PV construct between the 5'UTR and VP4 region, complementary sticky ends were produced at both the 5' end of the PV construct and the flanking regions the CFP_{PV} gene via Sal-I and Xho-I restriction digests. These complementary sticky ends served as docking sites that allowed site-specific insertion of the

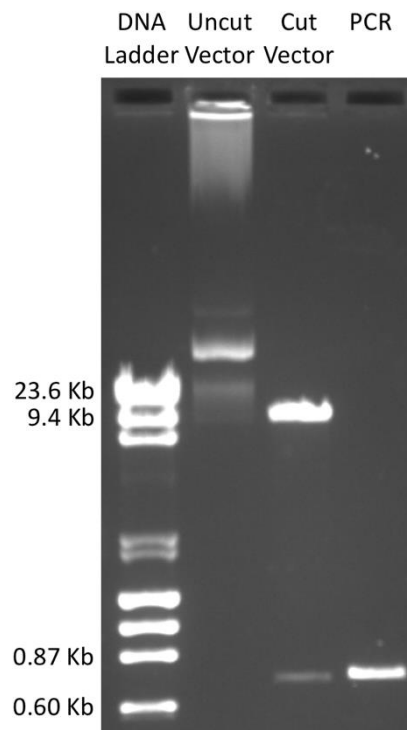


Figure 3. Sal-I & Xho-I Digest of CFP_{PV} gene and PV vector. Single bands were observed in both PCR and vector lanes, with no unexpected bands visible. Sal-I and Xho-I restriction enzymes were used for both digestion reactions. The faint band in the cut vector lane that corresponds to 0.7kb is the spill-over DNA from the PCR lane.

CFP_{PV} gene.

Gel result of the restriction digest shows two distinct, single vibrant bands in the cut vector lane and the CFP_{PV} PCR lane. With the exception of some spill-over DNA from the PCR lane into the cut vector lane, which forms a secondary faint band in the vector lane that matches

the size of the PCR product, there appears to be no unexpected DNA bands in the digested samples. This suggests that both the CFP_{PV} insert and the PV vector are completely digested. QIAEX purification is then performed to remove any left-over reagents from these samples.

Fusing the CFP_{PV} Gene into the PV Construct via Ligation

After the Sal-I and Xho-I digested CFP_{PV} gene and PV vector was purified, the PV vector was treated with SAP to remove the free phosphate groups on the digested vector, which prevented self-ligation between two digested vectors. In addition, this promoted ligation between the CFP_{PV} insert and the PV vector, since the CFP_{PV} fragments still contained free phosphate groups (necessary for ligation reaction). The digested fragments were then fused together via ligation to produce the CFP_{PV}-PV recombinant construct. DNA ligase was used to catalyze this reaction.

The ligation reaction generated a DNA form of the CFP_{PV}-PV recombinant construct, which can be transcribed into a functional reporter poliovirus RNA genome. As shown in figure 4, a spectrum of bands are visible in the “ligation product” lane whereas no such band is present in the “insert” lane, indicating self-ligation or multimerization between the CFP_{PV} insert. This also showed that the PCR fragments in the mixture were ligation active. No self-ligated vector was present in the mixture, demonstrating that the SAP treatment for vector was successful and complete. However, the gel result (figure 4) cannot definitively prove the existence of the recombinant plasmid, as the size of the ligated product is too similar to the empty vector for it to exhibit as a distinct band on the gel (around 5% difference).

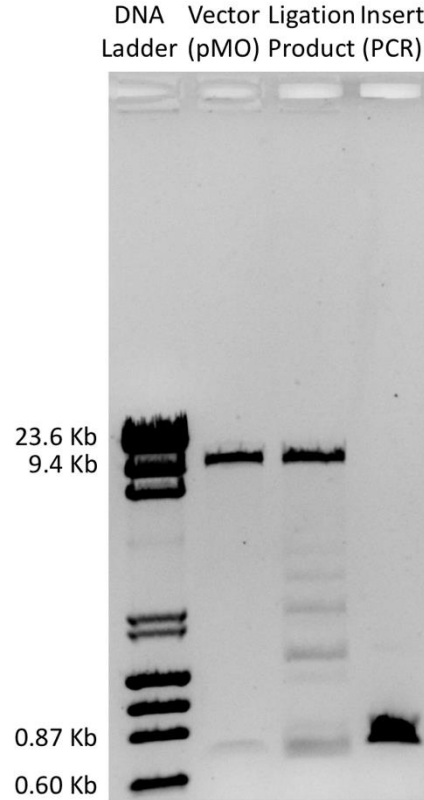


Figure 4. Ligation between the CFP_{PV} gene and the PV construct. A spectrum of bands is visible in the ligation product lane, indicating self-ligation or multimerization between the PCR gene inserts. No vector self-ligation band is visible, showing that the dephosphorylation of the vector was successful.

Selecting the Correct Ligation Product CFP_{PV}-PV: Transformation

Although the ligation was successful, it remains an issue to select out the correct ligation product from the reaction mixture. Only the CFP_{PV}-PV construct is desired in a mixture of empty vectors, CFP_{PV} inserts, self-ligated inserts, and the correct CFP_{PV}-PV plasmid. To do this, the reaction mixture was transformed into SURE (Stop Unwanted Rearrangement Events) competent cells. Because the vector construct contains antibiotic-resistance gene, cells that are successfully transformed with the CFP_{PV}-PV plasmid will survive and grow into colonies on an antibiotic

plate. On the other hand, because the un-ligated, linearized PV construct cannot enter the cells via transformation at high efficiency, the empty vectors cannot be used to produce antibiotic-resistant cells, thus will not produce large number of colonies on the antibiotic plate.

The resulting ligation product plate yielded around 25 colonies, while the control vector plate yielded only 3 colonies. The large number of colonies on the ligation product plate indicates that the recombinant plasmid CFP_{PV}-PV was successfully made and was transformed into SURE cells. The colonies were then selected out, inoculated, and screened to select and confirm the presence of the CFP_{PV}-PV.

Selecting the Correct Ligation Product CFP_{PV}-PV: Mini-Screen

To confirm the presence of the target plasmid CFP_{PV}-PV within the selected colonies on the antibiotic plate, DNA from various colonies on the ligation product plate was extracted via mini prep and screened via double digestion (Sal-I and Xho-I digest). Only the successfully ligated CFP_{PV}-PV construct could yield two DNA fragments on the gel using the same restriction enzymes that facilitated the targeted insertion of CFP_{PV} into PV vector. One fragment should match the size of the CFP_{PV} gene while the other matches with the PV vector. An accidental empty vector that entered the cell and facilitated its survival on the plate will not yield such two bands on the gel.

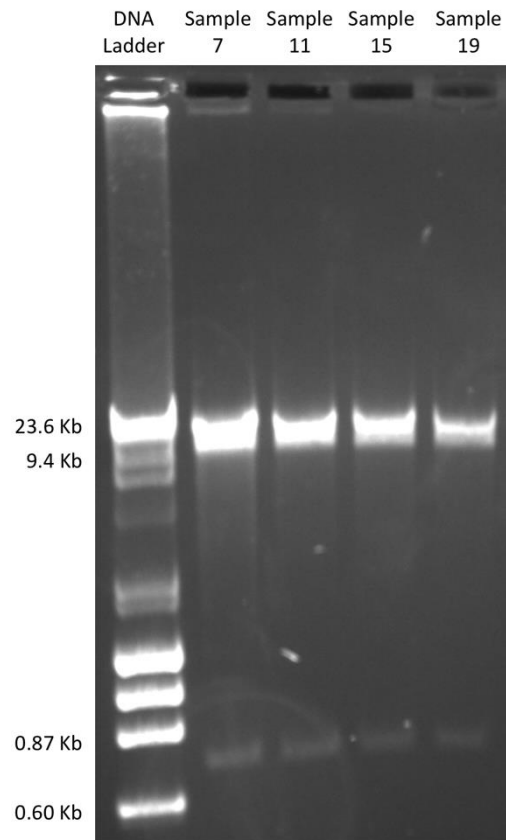


Figure 5. Sal-I and Xho-I Digest (MINI Screen). Four samples obtained from the ligation product plate yielded the characteristic double bands by digesting the extracted DNA with Sal-I and Xho-I. No unexpected bands are visible, showing that the CFP_{PV}-PV product is pure.

As shown in figure 5, four samples obtained from the ligation product plate yielded the characteristic double bands that root from digesting CFP_{PV}-PV construct with Sal-I and Xho-I enzymes. This indicates that the target CFP_{PV}-PV plasmid is successfully made and is ready to be used to produce the viral RNA genome. In addition, no unexpected bands were observed on the gel, which shows that the extracted CFP_{PV}-PV plasmid is pure.

Producing the Viral RNA Genome from the CFP_{PV}-PV DNA Construct

After confirming which samples within the colonies contain the correct CFP_{PV}-PV plasmid via screening, the plasmid was harvested from cells grown from these samples via midi prep. The plasmid was then linearized with Apa-1 enzyme before converting the DNA construct to RNA viral genome via T7 in vitro transcription. This prevented the RNA polymerase from keep transcribing the plasmid in a loop and enables it to dissociate from the plasmid after each round of transcription. T7 in vitro transcription was then performed to produce the viral RNA genome from the linearized CFP_{PV}-PV DNA construct. As shown in figure 6, a smear of RNA is

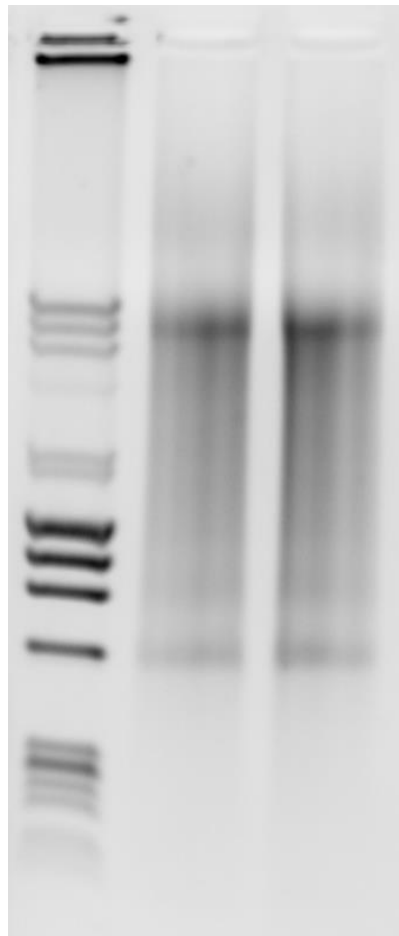


Figure 6. CFP_{PV}-PV RNA Viral Construct. RNA degradation can be seen from the smear on the gel. However, the target RNA construct was still successfully transcribed, as suggested by the bottom band that matches the expected size of the viral construct on the gel.

present on the gel, indicating that RNA degradation might have occurred during the transcription

process. However, target RNA construct was still successfully made, as suggested by the presence of the bottom band that matches the expected size of the recombinant viral construct on the gel, showing that the viral RNA was ready to be used to produce the fluorescent virus via transfection into HeLa cells.

Production and Detection of the Fluorescent Poliovirus CFP_{PV}-PV

The transcribed CFP_{PV}-PV RNA viral genome was then transfected into HeLa cells via electroporation to produce the reporter virus. Cells were seeded and transfected on a six-well plate. Cyan fluorescence was detected from the six-well plate after transfection and incubation, demonstrating the presence of the fluorescent virus.

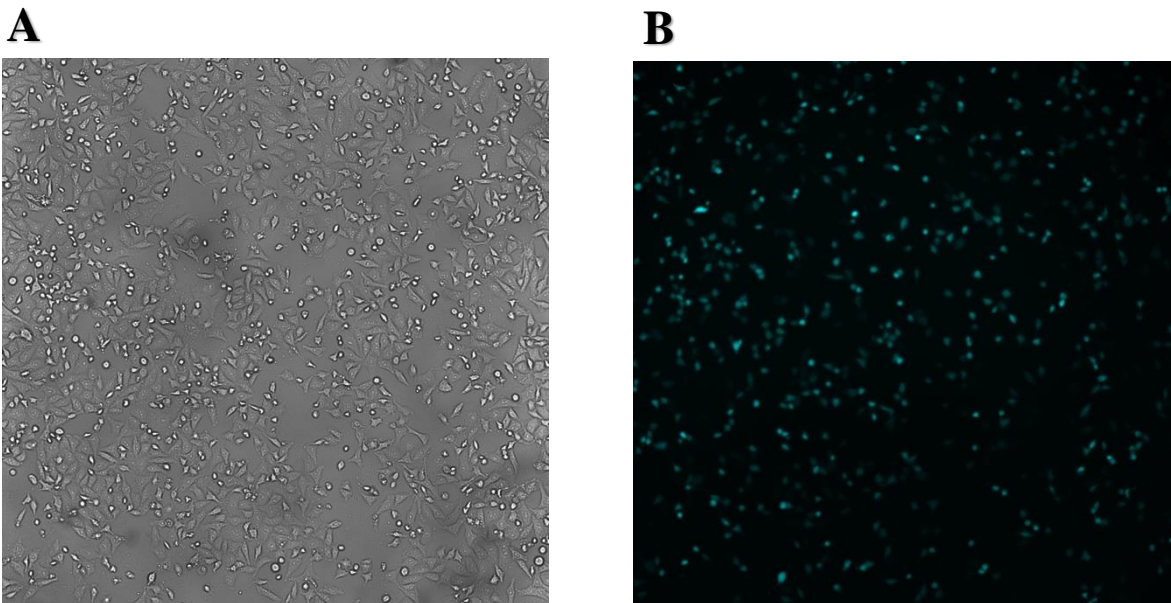


Figure 7. Bright Field and Fluorescent Imaging of the Cells. (A) Bright field imaging of the cells exhibits all the cells on the six-well plate. (B) Fluorescent imaging of the cells reveals only cells that contain fluorescent viruses.

As shown in figure 7 A and B, a large fraction of the cells exhibits cyan fluorescent signal, which was detected by the fluorescence microscope. This suggests that the engineered

viral RNA construct is functional and is capable of producing reporter viruses using HeLa cells as expected. The fluorescent virus was then harvested from the cells, purified, and stored as P0 stock for future use.

Characterization of the Reporter Virus Infectivity Using Plaque Assay

Although the reporter virus was proven to be capable of producing fluorescent signals as expected, it still remains a question whether the reporter gene affects the virus's infectivity compare to that of the wild type poliovirus. To ascertain this, a plaque assay was performed to quantify the infectivity of the fluorescent poliovirus.

As shown in figure 8, the viral titer is determined to be 1.1×10^8 PFU/mL for the reporter virus, which is consistent with that of the wild type poliovirus. This indicates that the CFP_{PV}

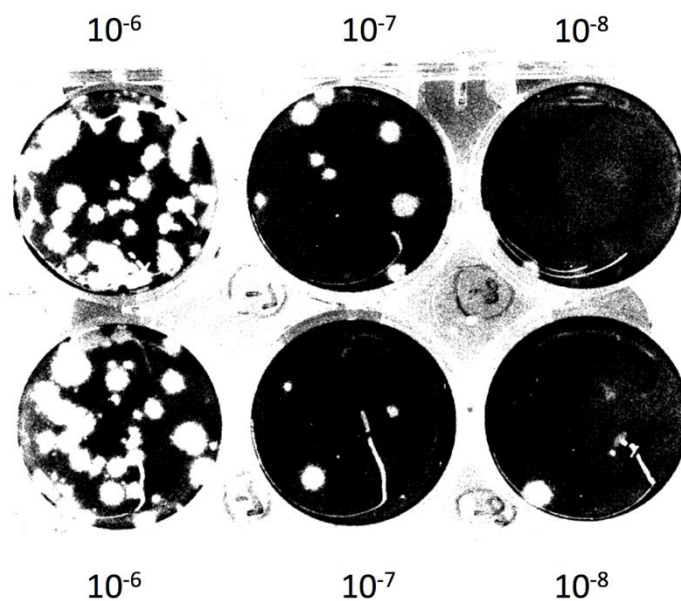


Figure 8. Plaque Assay. Plaque assay was performed to determine the viral titer of the fluorescent virus. Viral titer was determined to be 1.1×10^8 PFU/mL—similar to that of the wild type poliovirus.

gene inserted into the viral construct does not cause significant changes to the viral infectivity.

This

also shows that an infectious fluorescent reporter virus is successfully made and can be used for single cell analysis via fluorescence microscopy.

Chapter 5

Discussion

The goal of this study was to genetically engineer a reporter poliovirus whose fluorescent signal can be produced within a short duration upon infecting a cell. The purpose for designing such a virus is to enable investigation and characterization of the early events of poliovirus infection. This requires the new virus to be able to generate a fluorescent reporter that reflects the viral replication rate upon infection, retain wild type growth properties, and fluoresces faster than the currently available reporter virus designed in the Cameron lab. Ideally, the virus should generate fluorescent signal faster than 2-hour time point post infection, as this is when the initial viral translation phase occurs.

As the initial characterizations shows, the engineered new fluorescent reporter virus met most of our original expectations. For example, robust fluorescent signal was detected from cells upon infection (Fig. 7B); the virus's growth properties were on par with that of the wild type poliovirus (Fig. 8); moreover, results from a related fluorescent virus shows that the fluorescent rate of viruses created by this construct is improved from the currently available reporter virus in the Cameron lab. These traits suggest that the fluorescent reporter virus that we aimed to produce was successfully made.

This newly constructed virus can be used to develop single-step growth curves using a fluorescent microscope. In addition, a microfluidic chip can be utilized to enable visualization of each infection event that occurs in individual cells, allowing distinct traits of viral infection in different cells to be unraveled.³⁴

The cyan-fluorescent virus produced in this study can also be used in conjunction with a green-fluorescent virus or a red-fluorescent virus to conduct co-infection studies. By infecting cells with two viruses of different colors and use of a fluorescent microscope to track the growth rate of the both viruses, limiting factors that restricts the extent of poliovirus infection can be determined. For example, if two viruses within an individual cell exhibit different growth rate at a certain time point post infection, it can be concluded that the viral factor, instead of the host cell factor, is playing the dominant role at determining the viruses' infectivity. This is because the host cell factor would place the same effect on both viruses within the cell, thus causing in the viruses' to replicate with similar characteristics growth rate.⁴³ Therefore, any difference in viral infection rate at this particular phase must be caused by viral factors, such as viral genomic variation or stochastic viral gene expression. On the other hand, if the two viruses that co-infected the same cell exhibit different growth rates at a certain phase, it can be concluded that it is the host cell factor, instead of the viral factor, that is playing the dominant role at determining the viruses' infectivity. Viral factor is eliminated from this scenario because the two viruses in the same cell is replicating at the same rate, indicating that the viral factor is not causing the viruses to behave differently in cells. However, if viruses in different cells still exhibit different growth rate, it suggests that this variation in viral infection can be attributed to differences in host cell factors within different individual cells.¹¹ As can be seen, the advantage of using co-infection is that it helps eliminate the infection variability caused by host cell factors by

providing the two viruses with the same host cell environment. However, to employ this method, reporter viruses that can fluoresce at different colors must be engineered. Since a green-fluorescent poliovirus is already available in the Cameron lab, designing a cyan-fluorescent virus becomes desirable for such purpose.

Although this newly designed virus is proved to be an improvement according to the initial characterizations, an issue still lingers. As mentioned before, we expected that in addition to designing a reporter virus that fluoresces blue upon infection, the fluorescent signal should also be generated within a 2-hour time point post infection, as this would allow us to investigate the early viral infection events that occur at this time. However, our initial characterization shows that although the fluorescent rate of this blue virus is improved compared to the green virus that was already available in the lab, its fluorescent rate still wasn't matching our expectation. This indicates that the virus is still experiencing a minor fluorescent delay. We suspect that this delay is due to a lack of linkage distance between the CFP_{PV} and the VP4 regions on the genome. This short linkage distance between the two regions will likely diminish the CFP's protein folding efficiency upon translation due to the steric strain between CFP and VP4.³⁵ Moreover, the short linkage distance will limit the access of the 3C^{PRO} viral protease at the linkage, preventing 3C^{PRO} from efficiently releasing the CFP from the viral polypeptide via cleavage. Since being in an unbound state is critical to improving the fluorescent rate of the CFP, as it allows the protein to better immerse in an aqueous environment and facilitate protein folding, this lack of efficient 3C^{PRO} cleavage at the CFP_{PV}-VP4 linkage region leads to fluorescent delay.^{36, 37}

Chapter 6

Future Directions

As mentioned in the last section, the newly designed reporter virus still experiences a minor fluorescent delay, which makes further improvement on the fluorescent rate an imminent topic. To make such improvement, one approach is already underway. Since the suspected cause for the fluorescent delay is a lack of linkage distance between the CFP_{PV} and VP4 regions, we propose to resolve this issue by adding a linker region (~90nt) in between. This would effectively increase the linkage distance, reducing the steric between the CFP and VP4 proteins within the polypeptide and allow the CFP to have more room fold. In addition, this gives the 3C^{pro} more access to the cleavage site at the linkage region, enabling the CFP to be released more quickly via cleavage.

Therefore, adding the linker region between CFP_{PV} and VP4 regions would further improve the fluorescent rate of the virus by enabling the CFP to fold more efficiently and allowing it to be released more quickly.

Another approach to this is to add a 2A self-cleaving peptide in between the CFP_{PV} and VP4 regions. 2A is an oligopeptide that is found between adjacent viral proteins in certain members of the picornavirus family.³⁸ It is able to undergo self-cleavage to release mature viral proteins from the viral polypeptide via a post-translational effect known as “stop-go” or “stop-carry”.^{39, 40} The advantage of utilizing this peptide in between the CFP_{PV} and VP4 regions is that it enables an immediate cleavage that releases the CFP upon translation without the involvement of any viral protease.⁴¹ Since the fluorescent delay that past reporter viruses have encountered are mainly attributed to slow viral protease-mediated cleavage, removing this step from the

process by using 2A could significantly improve the fluorescent protein maturation rate and subsequently improve the fluorescent rate of the virus.

BIBLIOGRAPHY

1. Modrow, S., Falke, D., Truyen, U., Schätzl, H., (2013), Viruses with Single-Stranded, Positive-Sense RNA Genomes. *Molecular virology*. Berlin, Heidelberg: Springer Berlin Heidelberg. pp. 185–349. ISBN 978-3-642-20718-1.
2. Nagy, P., Pogany, J., (2011), The dependence of viral RNA replication on co-opted host factors. *Nature Reviews. Microbiology*, 10 (2): 137–149.
doi:10.1038/nrmicro2692. PMID 22183253.
3. Simon-Loriere, E., & Holmes, E. C. (2011). Why do RNA viruses recombine? *Nature Reviews. Microbiology*, 9(8), 617–626. <http://doi.org/10.1038/nrmicro2614>
4. Koonin, E. V., Senkevich, T. G., & Dolja, V. V. (2006). The ancient Virus World and evolution of cells. *Biology Direct*, 1, 29. <http://doi.org/10.1186/1745-6150-1-29>
5. Rybicki, EP. (1990) The classification of organisms at the edge of life, or problems with virus systematics. *South African Journal of Science*. 86,182–186.
6. Sanjuan, R., Nebot, M. R., Chirico, N., Mansky, L. M., Belshaw, R. (2010). Viral Mutation Rates. *Journal of Virology*. 84 (19): 9733–9748. doi:10.1128/JVI.00694-10. ISSN 0022-538X.
7. Domingo, E. (2002). Quasispecies Theory in Virology. *Journal of Virology*. vol. 76 no. 1 463-465. doi: 10.1128/JVI.76.1.463-465.2002
8. Domingo, E., and Holland, J.J., (1997), RNA virus mutations and fitness for survival. *Annu. Rev. Microbiol.*, 51, 151-178

9. Wilkinson, D. J. Stochastic modelling for quantitative description of heterogeneous biological systems. *Nature Rev. Genet.* 10, 122–133 (2009)
10. Kew, O., Sutter, R., Gourville, E., Dowdle, W., and Pallansch, M., (2005), *Annual Review of Microbiology.*, 59:1, 587-635
11. Guo, F., Li, S., Caglar, M., (2017), Single-Cell Virology: On-Chip Investigation of Viral Infection Dynamics. *Cell Reports.*, 21, 1692-1704
12. Ryan KJ, Ray CG, eds. (2004). *Sherris Medical Microbiology* (4th ed.). McGraw Hill. ISBN 0-8385-8529-9.
13. Hogle, J. (2002). Poliovirus cell entry: common structural themes in viral cell entry pathways. *Annu Rev Microbiol.* 56: 677–702.
doi:10.1146/annurev.micro.56.012302.160757. PMC 1500891. PMID 12142481
14. Pelletier J, Sonenberg N (1988). Internal initiation of translation of eukaryotic mRNA directed by a sequence derived from poliovirus RNA. *Nature.* 334 (6180): 320–5.
doi:10.1038/334320a0. PMID 2839775
15. Jang SK, Kräusslich HG, Nicklin MJ, Duke GM, Palmenberg AC, Wimmer E (1988). A segment of the 5' nontranslated region of encephalomyocarditis virus RNA directs internal entry of ribosomes during in vitro translation. *J. Virol.* 62 (8): 2636–43. PMC 253694. PMID 2839690
16. John Carter; Venetia A. Saunders (2007). *Virology: Principles and Applications*. John Wiley & Sons. p. 165. ISBN 978-0-470-02386-0
17. Harper, David R. (2012). *Viruses: Biology, Applications, and Control*. The United States of America: Garland Science. p. 57. ISBN 978-0-8153-4150-5

18. Novoa, I., & Carrasco, L. (1999). Cleavage of Eukaryotic Translation Initiation Factor 4G by Exogenously Added Hybrid Proteins Containing Poliovirus 2A^{pro} in HeLa Cells: Effects on Gene Expression. *Molecular and Cellular Biology*, 19(4), 2445–2454
19. Barco, A., Feduchi, E., & Carrasco, L. (2000). A Stable HeLa Cell Line That Inducibly Expresses Poliovirus 2A^{pro}: Effects on Cellular and Viral Gene Expression. *Journal of Virology*, 74(5), 2383–2392.
20. Kaiser, C., Dobrikova, E. Y., Bradrick, S. S., Shveygert, M., Herbert, J. T., & Gromeier, M. (2008). Activation of cap-independent translation by variant eukaryotic initiation factor 4G in vivo. *RNA*, 14(10), 2170–2182.
<http://doi.org/10.1261/rna.1171808>
21. Castelló, A., Álvarez, E., & Carrasco, L. (2011). The Multifaceted Poliovirus 2A Protease: Regulation of Gene Expression by Picornavirus Proteases. *Journal of Biomedicine and Biotechnology*, 2011, 369648. <http://doi.org/10.1155/2011/369648>
22. Leong LEC, Cornell CT, Semler BL. Processing determinants and functions of cleavage products of picornavirus polyproteins. In: Semler BL, Wimmer E, editors. *Molecular Biology of Picornaviruses*. Washington, DC, USA: ASM Press; 2002. pp. 187–198.
23. Lee CK, Wimmer E. Proteolytic processing of poliovirus polyprotein: elimination of 2A(pro)-mediated, alternative cleavage of polypeptide 3CD by in vitro mutagenesis. *Virology*. 1988;166(2):405–414.
24. Herold, J., & Andino, R. (2000). Poliovirus Requires a Precise 5' End for Efficient Positive-Strand RNA Synthesis. *Journal of Virology*, 74(14), 6394–6400.

25. Daijogo, S., Semler, B. (2011). Mechanistic Intersections Between Picornavirus Translation and RNA Replication. *Advances in Virus Research*. Academic Press; 2011. Vol 80. pp. 1-24
26. Novak JE, Kirkegaard K. Coupling between genome translation and replication in an RNA virus. *Genes & Dev*. 1994; 8:1726–1737.
27. Gamarnik, A. V., & Andino, R. (1998). Switch from translation to RNA replication in a positive-stranded RNA virus. *Genes & Development*, 12(15), 2293–2304.
28. John Carter; Venetia A. Saunders (2007). *Virology: Principles and Applications*. John Wiley & Sons. p. 166. ISBN 978-0-470-02386-0.
29. Kew O, Sutter R, de Gourville E, Dowdle W, Pallansch M (2005). Vaccine-derived polioviruses and the endgame strategy for global polio eradication. *Annu Rev Microbiol*. 59: 587–635. doi:10.1146/annurev.micro.58.030603.123625. PMID 16153180.
30. Altschuler, Steven J.; Wu, Lani F. (2010). Cellular Heterogeneity: Do Differences Make a Difference?. *Cell*. 141 (4): 559–563. doi:10.1016/j.cell.2010.04.033. ISSN 0092-8674. PMC 2918286. PMID 20478246
31. Enquist, L. W., & for the Editors of the Journal of Virology. (2009). Virology in the 21st Century. *Journal of Virology*, 83(11), 5296–5308.
<http://doi.org/10.1128/JVI.00151-09>
32. Schulte, M.B. and Andino, R. (2014). Single-cell analysis uncovers extensive biological noise in poliovirus replication. *J. Virol*. 2014; 88: 6205–6212

33. Akpınar, F., Timm, A., and Yin, J. (2015). High-throughput single-cell kinetics of virus infections in the presence of defective interfering particles. *J. Virol.* 2015; 90: 1599–1612
34. Seah, Y.F., Hu, H., Merten, C.A. (2018). Microfluidic single-cell technology in immunology and antibody screening. *Molecular Aspects of Medicine*. Vol 59. pp. 47-61
35. Ellis RJ (July 2006). Molecular chaperones: assisting assembly in addition to folding. *Trends in Biochemical Sciences*. 31 (7): 395–401. doi:10.1016/j.tibs.2006.05.001. PMID 16716593
36. Pratt C, Cornely K (2004). "Thermodynamics". *Essential Biochemistry*. Wiley. ISBN 978-0-471-39387-0. Retrieved 2016-11-26.
37. van den Berg B, Wain R, Dobson CM, Ellis RJ (August 2000). Macromolecular crowding perturbs protein refolding kinetics: implications for folding inside the cell. *The EMBO Journal*. 19 (15): 3870–5. doi:10.1093/emboj/19.15.3870. PMC 306593. PMID 10921869.
38. Ryan, M.D., King, A.M. & Thomas, G.P (1991). Cleavage of foot-and-mouth disease virus polyprotein is mediated by residues located within a 19-amino acid sequence. *The Journal of General Virology.*, 72, (Pt 11), 2727–2732.
39. Wang, Y. *et al* (2015). 2A self-cleaving peptide-based multi-gene expression system in the silkworm *Bombyx mori*. *Scientific Reports.*, 5, 16273
40. Donnelly M, Luke G, Mehrotra A, Li X, Hughes L, Gani D, Ryan M. J. (2001). Analysis of the aphthovirus 2A/2B polyprotein ‘cleavage’ mechanism indicates not a

- proteolytic reaction, but a novel translational effect: a putative ribosomal 'skip' *Gen. Virol.* 82(5):1013-1025 doi:10.1099/0022-1317-82-5-1013
41. Donnelly, M. L. L., Gani, D., Flint, M., Monaghan, S. & Ryan, M. D. (1997). The cleavage activity of aphtho- and cardiovirus 2A proteins. *Journal of General Virology* 78, 13-21.
42. Wuitschick JD, Karrer KM. (1999). Analysis of genomic G + C content, codon usage, initiator codon context and translation termination sites in *Tetrahymena thermophila*. *J. Eukaryot. Microbiol.* 46 (3): 239–47. doi:10.1111/j.1550-7408.1999.tb05120.x. PMID 10377985.
43. Susi, H., Barres, B., Vale, P. F., & Laine, A. (2015). Co-infection alters population dynamics of infectious disease. *Nature Communications* 6. Article number: 5975. doi:10.1038/ncomms6975

ACADEMIC VITA

Ziwei Yang

436 Canterbury Drive State College, PA 16803 (570)9854920 zqy5103@psu.edu

Education

The Pennsylvania State University, Schreyer Honors College, University Park, PA

B.S. in Biochemistry and Molecular Biology

Honors in Biochemistry and Molecular Biology

Graduation Date: May, 2018

Honors and Awards

Gruber Science Fellowship, Yale University	2018
Arthur K. Anderson Memorial Award	2017
Schreyer Honors College Research Grant, Penn State	2017
Charles and Vickie Grier Undergraduate Research Fund	2017
Edward B Nelson Undergraduate Research Fund	2017
Paul and Mildred Berg Endowed Undergraduate Research Fund	2017
The Evan Pugh Scholar Senior Award, Penn State	2017
The President Sparks Award, Penn State	2016
The President's Freshman Award, Penn State	2015
Academic Achievement Incentive Scholarship, Penn State	2014
The Honor Society of Phi Kappa Phi	(2017 – present)
Golden Key International Honour Society	(2017 – present)
Dean's List	(2014 – 2018)

Professional Membership

American Society for Biochemistry and Molecular Biology

American Society for Virology

American Association for the Advancement of Science

Research Experience

Honors Independent Research (Thesis Research) Summer 2017 – Present

Principal Investigator: Dr. Craig E. Cameron, Professor and Eberly Family Chair of Biochemistry and Molecular Biology at The Pennsylvania State University

Research Project: Investigating the cell-to-cell variability of poliovirus infection using single-cell analysis

- Engineered a cyan fluorescent reporter-expressing poliovirus that generates fluorescent signal upon viral translation and that retains wild type growth properties—a CFP-expressing Poliovirus (CFP-PV)
- Performed initial characterizations of the engineered CFP-PV

- Prepared CFP-PV virus stock to assist other research carried out in the laboratory, such as co-infection studies
- Monitored the kinetics of the cyan fluorescence of the CFP-poliovirus via plate reader and the kinetics of the viral RNA production via q-PCR

Research Assistant, The Pennsylvania State University August 2015 – May 2016
Principal Investigator: Dr. Lee J. Silverberg, Associate Professor of Chemistry at Penn State Schuylkill

Research Project: Synthesis of biologically active compounds that could aid in the development of therapeutic drugs

- Assisted in the organic synthesis of novel heterocyclic compound—rac-2,3-diphenyl-2,3,5,6-tetrahydro-4H-1,3-thiazin-4-one 1-oxide—a six-membered heterocycle with a wide range of biological activity
- Synthesized four other biologically active compounds, including 3-aryl-2-phenyl-2,3-dihydro-4H-1,3-benzo-thia-zin-4-ones & 2-aryl-3-phenyl-2,3-dihydro-4H-1,3-benzothiazin-4-ones
- Help investigated the chemical structures of the synthesized heterocyclic compounds using UV spectroscopy

Publications

- Yennawar, H. P., Noble, D. J., **Yang, Z.**, and Silverberg, L. J. “rac-2,3-Diphenyl-2,3-dihydro-4H-pyrido[3,2-e]- [1,3] thiazin-4-one 1-oxide.” *IUCrData*, 2017, DOI: 10.1107/S2414314617011129
- Yennawar, H. P., Fox, R., Moyer, Q. J., **Yang, Z.**, and Silverberg, L. J. “Crystal structure of 2,3-di-phenyl-2,3-di-hydro-4H-1,3-benzo-thia-zin-4-one 1-oxide.” *Acta Crystallographica Section E: Crystallographic Communications*, 2017, DOI: 10.1107/S2056989017010313
- Yennawar, H. P., **Yang, Z.**, and Silverberg, L. J. “Crystal structure of rac-2,3-diphenyl-2,3,5,6-tetrahydro-4H-1,3-thiazin-4-one 1-oxide.” *Acta Crystallographica Section E: Crystallographic Communications*, 2016, DOI: 10.1107/S2056989016015395
- Yennawar, H. P., Coyle, D. J., Noble, D. J., **Yang, Z.**, and Silverberg, L. J. “Crystal structures of three substituted 3-aryl-2-phenyl-2,3-di-hydro-4H-1,3-benzo-thia-zin-4-ones.” *Acta Crystallographica Section E: Crystallographic Communications*, 2016, DOI: 10.1107/S2056989016011002
- Silverberg, L. J., Pacheco, C., Lagalante, A., Tierney, J., Bachert, J. T., Bayliff, J. A., Bendinsky, R. V., Cali, A. S., Chen, L., Cooper, A. D., Minehan, M. J., Mroz, C. R., Noble, D. J., Weisbeck, A. K., Xie, Y., and **Yang, Z.** “Synthesis and spectroscopic properties of a series of novel 2-aryl-3-phenyl-2,3-dihydro-4H-1,3-benzothiazin-4-ones.” *Acta Crystallographica Section E: Crystallographic Communications*, 2016, DOI: <http://dx.doi.org/10.3998/ark.5550190.p009.875>

Presentation

Construction and Characterization of a CFP-Expressing Poliovirus

- Research Experience for Undergraduates Program (REU) Poster Session, July 2017
- 7th American Chemical Society Annual Undergraduate Poster Symposium (Central Pa Local Section), September 2017
- 10th Annual Postdoc Research Exhibition at Penn State, September 2017 (postdoc as mentor and undergraduate as mentee co-present result)
- Penn State Eberly College of Science Poster Exhibition, October 2017
- Undergraduate Research Symposium in the Chemical and Biological Sciences at University of Maryland, October 2017

Synthesis and Crystal Structure of *rac*-2,3-diphenyl-2,3,5,6-tetrahydro-4H-1,3-thiazin-4-one 1-oxide

- Undergraduate Research Symposium at Penn State Schuylkill, April 2016

Synthesis and Crystal Structure of three substituted 3-aryl-2-phenyl-2,3-dihydro-4H-1,3-benzothiazin-4-ones

- Undergraduate Poster Conference at Penn State Schuylkill, December 2015

Skills

Laboratory Skills:

- Cell Culture (mammalian and bacteria)
- Gel Electrophoresis (DNA and RNA) and SDS-PAGE
- 400 MHz NMR spectroscopy (H^1 and C^{13})
- Infrared Spectroscopy
- NanoDrop Microvolume Quantitation of Nucleic Acids
- Live Cell Imaging via Fluorescence Microscopy
- PCR cloning
- Mini-Prep, Midi-Prep, and Mini-Screen
- Viral Infection, DNA Transformation, RNA Transfection, Plaque Assay
- DNA, RNA, Protein, and Virus purification
- Cell Count using Hemocytometer
- Western Blot

Languages:

- English (fluent)
- Chinese (fluent)

Extracurricular Activities

Penn State Schuylkill Campus Honors Society, Vice President

2015 – 2016

- Coordinated weekly meetings
- Recorded meetings and reported progress
- Organized honors society events—such as networking with distinguished faculty/alumni

Penn State Schuylkill Student Government, Diversity & Equity Representative 2015 – 2016

- Addressed students' concerns regarding cultural diversity on campus to the student government cabinet
- Co-designed and helped implemented programs/events that promotes cultural diversity on Schuylkill campus

Lion Ambassador

2015 – 2017

- Led tours for prospective students and families
- Participated in Open House Events and Outreach Events
- Networked with distinguished faculty/alumni